Science Advances
AAAS

advances.sciencemag.org/cgi/content/full/5/6/eaaw2844/DC1

Supplementary Materials for

High-resolution, reconfigurable printing of liquid metals with three-dimensional structures

Young-Geun Park, Hyeon Seok An, Ju-Young Kim, Jang-Ung Park*

*Corresponding author. Email: jang-ung@yonsei.ac.kr

Published 21 June 2019, *Sci. Adv.* **5**, eaaw2844 (2019)
DOI: 10.1126/sciadv.aaw2844

The PDF file includes:

Fig. S1. SEM images of the kinked or bent regions of the printed EGaIn filaments.
Fig. S2. The lift-off or cutoff state of line versus the nozzle lift-off velocity.
Fig. S3. Photograph of lift-off of EGaIn during reconfiguration.
Fig. S4. Formation of kink- or arc-shaped 3D structures by reconfiguration.
Fig. S5. Electrical breakdown test of EGaIn.
Fig. S6. Heat resistance of EGaIn 3D structures.
Fig. S7. SEM images of soft encapsulation of EGaIn by parylene.
Fig. S8. Contact angle between EGaIn and Au.
Fig. S9. The efficiency of interconnection through 3D printing.
Table S1. Comparison with conventional 3D printing techniques of conductive materials in the aspect of printable materials, resolution, reconfigurability, processing temperature, and conductivity.
Table S2. Comparison with published results of liquid metal patterning in the aspect of line width, the free-standing 3D structure, reconfigurability, and the used substrate.
Legends for movies S1 to S10

Other Supplementary Material for this manuscript includes the following:

(available at advances.sciencemag.org/cgi/content/full/5/6/eaaw2844/DC1)

Movie S1 (.avi format). Reconfiguration of the square coil antenna.
Movie S2 (.avi format). Multiple reconfigurations of the EGaIn filament.
Movie S3 (.avi format). Reconfiguration of EGaIn that connects about a 650-µm step.
Movie S4 (.avi format). Formation of kink-shaped 3D structure by reconfiguration.
Movie S5 (.avi format). Formation of arc-shaped 3D structure by reconfiguration.
Movie S6 (.avi format). Breakdown procedure of EGaIn under increasing dc bias.
Movie S7 (.avi format). Breakdown procedure of EGaIn under increasing ac bias (120 Hz).
Movie S8 (.avi format). Lift-off and relocation of 3D interconnect for LED switching circuit.

Movie S9 (.avi format). Light emission from the RGB LED array.
Movie S10 (.avi format). Light emission from selected pixels in the 4 × 4 microLED array.

Supplementary Materials

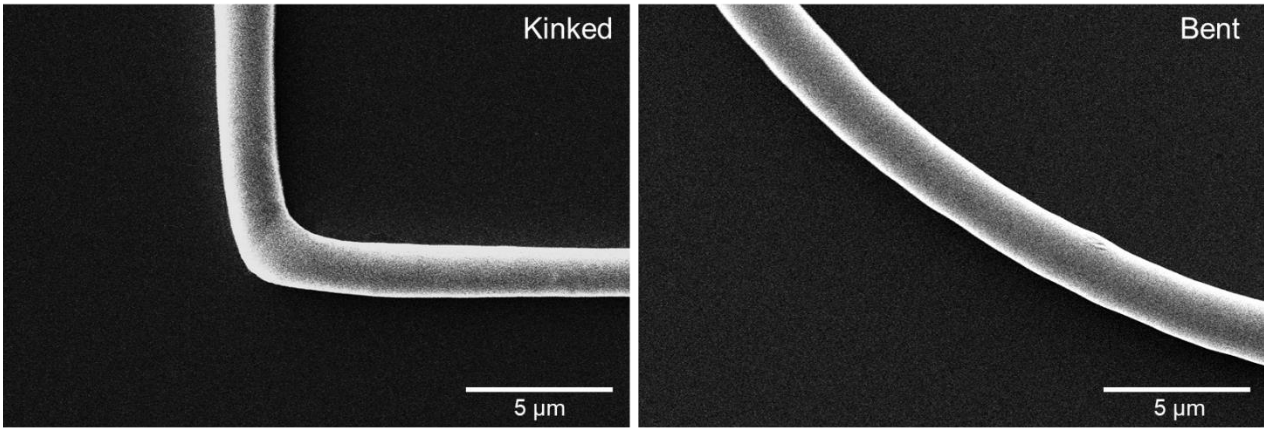

Fig. S1. SEM images of the kinked or bent regions of the printed EGaIn filaments. The uniformity in line width is not significantly changed at the corner of the kinked or bent patterns.

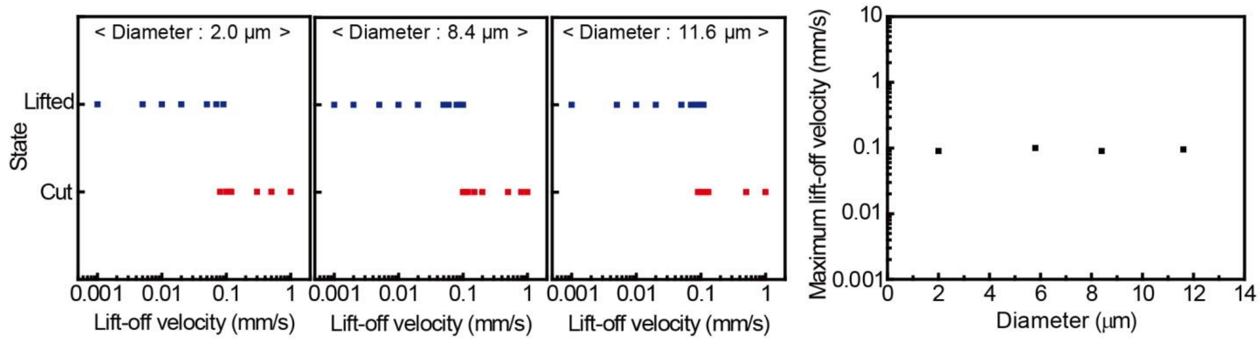

Fig. S2. The lift-off or cutoff state of line versus the nozzle lift-off velocity. Maximum lift-off velocities are about 0.1 mm/s for the diameters of filaments from 2.0 to 11.6 μm.

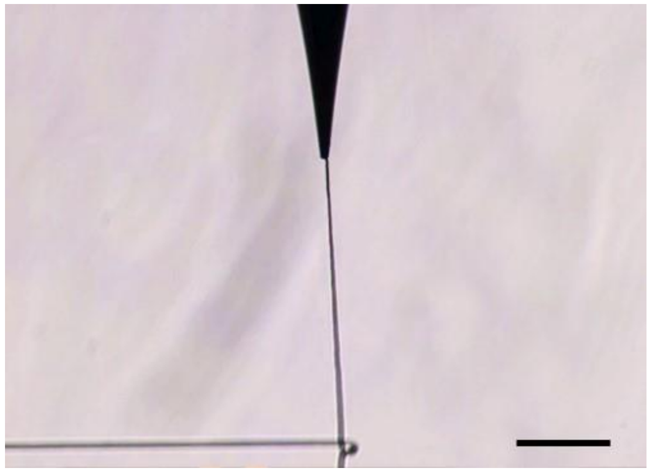

Fig. S3. Photograph of lift-off of EGaIn during reconfiguration. Preprinted EGaIn of 8 μm line width is lifted up to 2 mm. Scale bar, 500 μm. Photo Credit: Young-Geun Park, Yonsei University.

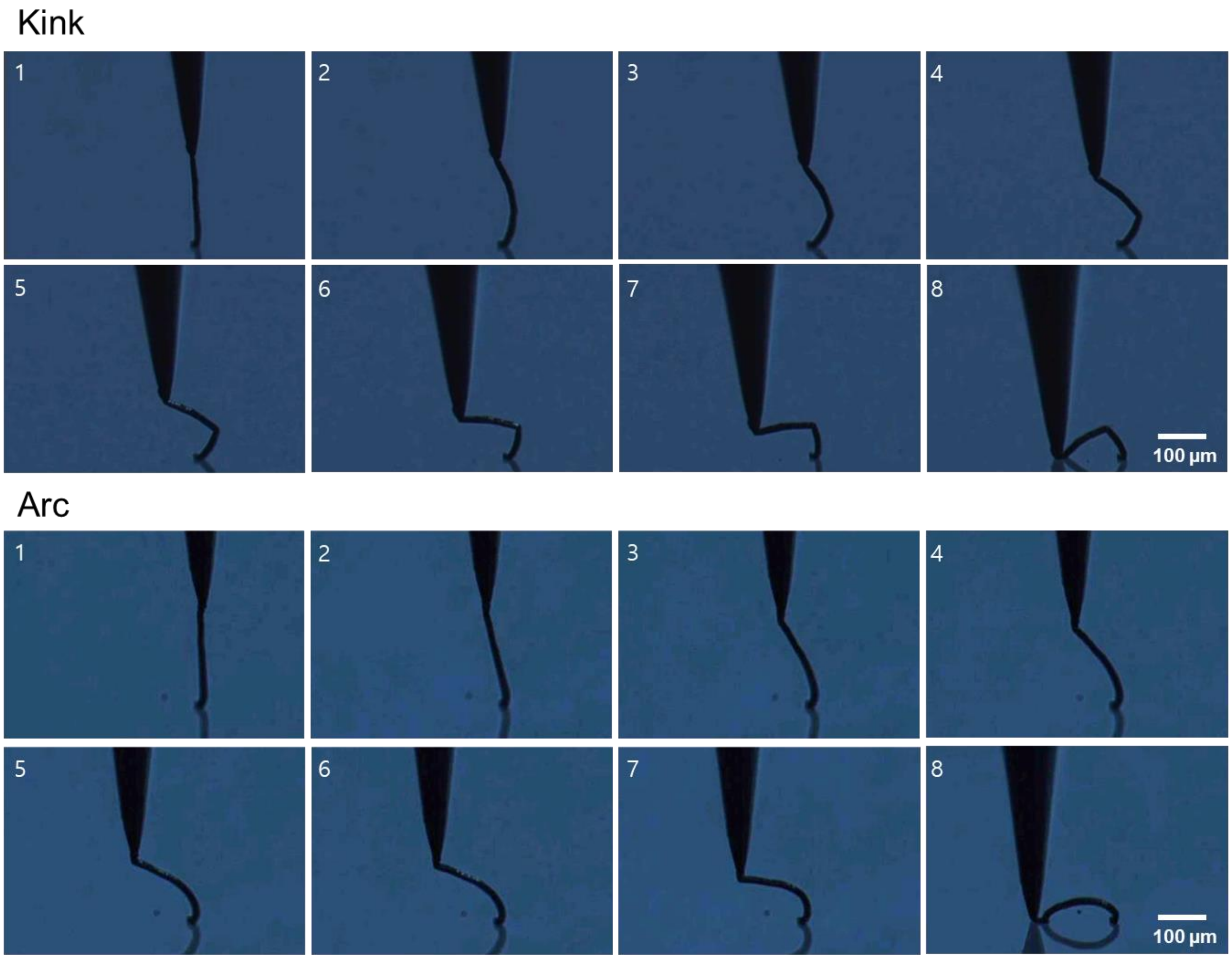

Fig. S4. Formation of kink- or arc-shaped 3D structures by reconfiguration.

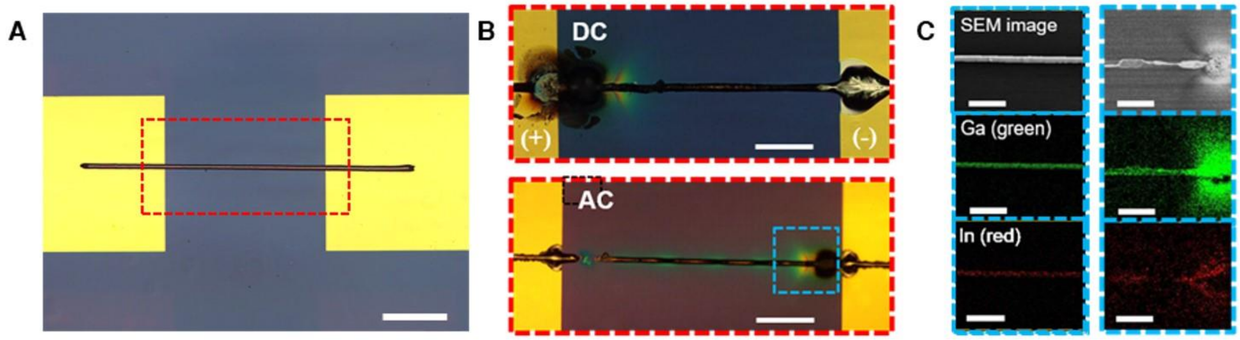

Fig. S5. Electrical breakdown test of EGaIn. (**A**) Optical micrograph of EGaIn electrode printed across two Au contact pads. Scale bar, 200 μm. (**B**) Optical micrograph of EGaIn electrode after a breakdown by dc or ac electric fields. Scale bars, 100 μm. (**C**) SEM image and EDS analyses of EGaIn electrode before breakdown (left) and after breakdown (right), at the blue dotted square in (B). Scale bars, 50 μm.

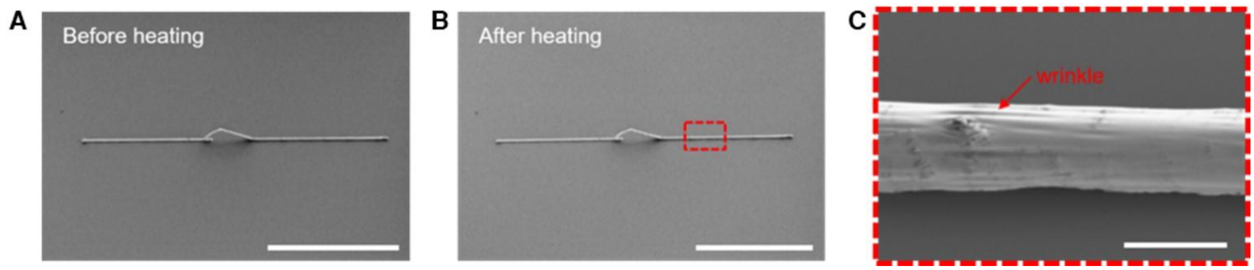

Fig. S6. Heat resistance of EGaIn 3D structures. (**A**) SEM image of 3D structure of printed EGaIn before heating. Scale bar, 500 µm. (**B**) SEM image of 3D structure of EGaIn after heated 30 minutes at 500 °C. Scale bar, 500 µm. (**C**) Enlarged SEM image of EGaIn line marked in (B). Scale bar, 10 µm.

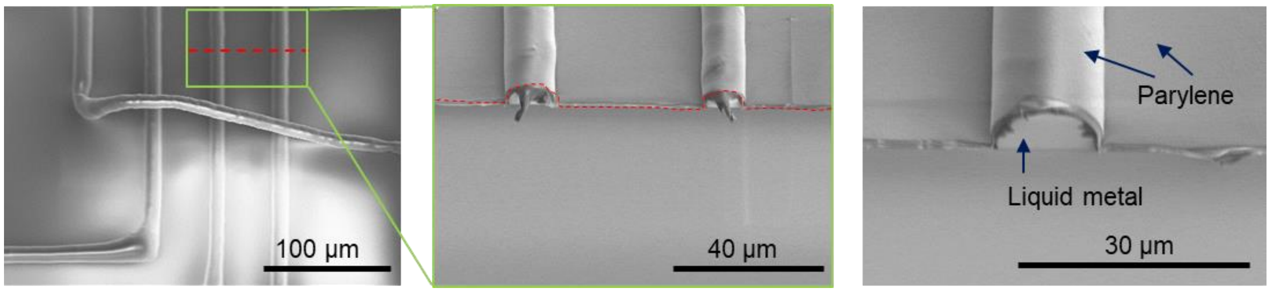

Fig. S7. SEM images of soft encapsulation of EGaIn by parylene. 3D printed EGaIn line is conformally encapsulated with parylene. The thickness of deposited parylene was 500 nm.

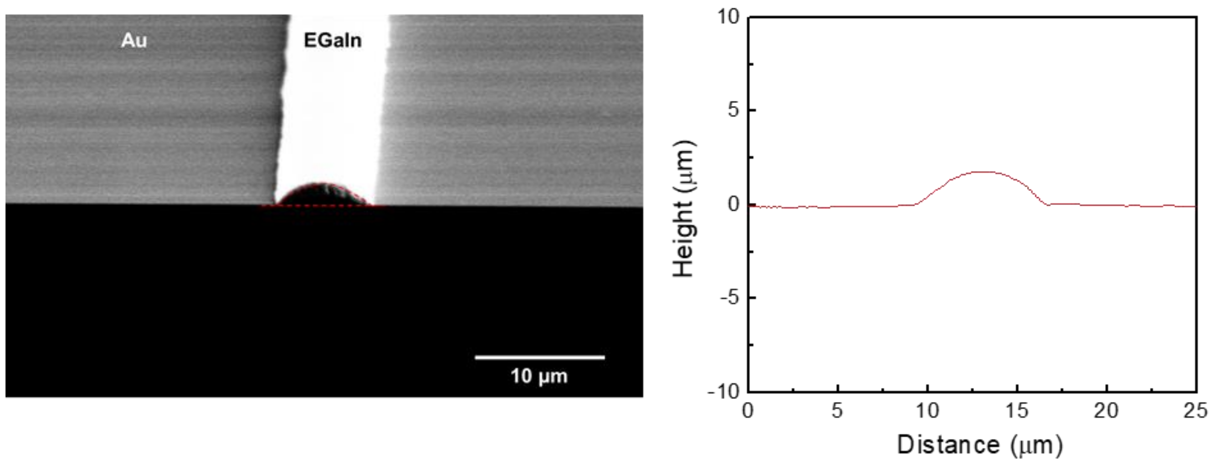

Fig. S8. Contact angle between EGaIn and Au. SEM image (left) of the direct-printed EGaIn filament on Au and its AFM cross-sectional profile (right). The contact angle between this filament and Au pad is about 30°, which is comparable to the previous study on the contact angle between the oxide-removed liquid metal and Au (*40*). These results suggest that the oxide formation is negligible for the direct printing case.

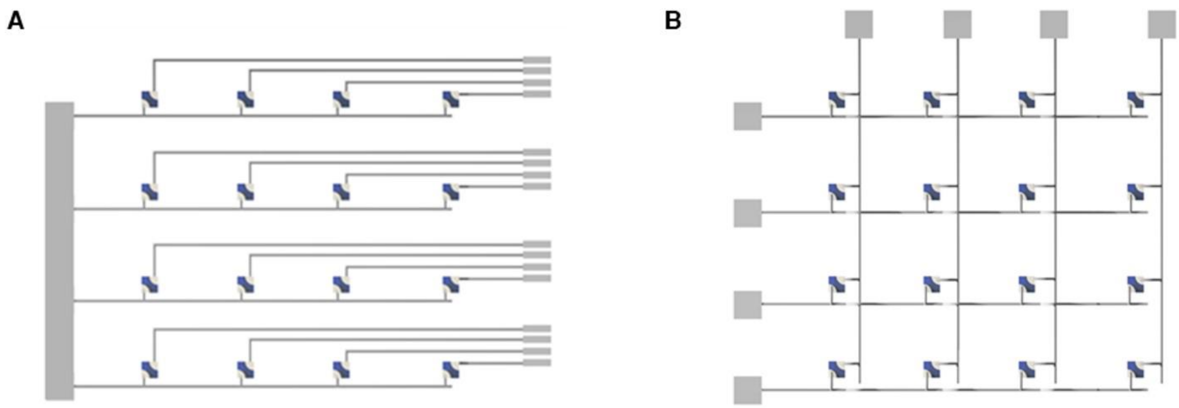

Fig. S9. The efficiency of interconnection through 3D printing. (**A**) Schematic illustration of a 4 × 4 array of LEDs with 2D interconnects. (**B**) Schematic illustration of a 4 × 4 array of LEDs with 3D interconnects.

Table S1. Comparison with conventional 3D printing techniques of conductive materials in the aspect of printable materials, resolution, reconfigurability, processing temperature, and conductivity. RT=Room temperature.

	Printable Materials	Resolution	Reconfigurability	Processing temperature	Conductivity (S/μm)	Ref.
This work	Liquid metal	1.9 μm (diameter)	O	RT	3.4	-
Direct printing	Liquid metal	340 μm (diameter)	X	RT	3.4	(*24*)
	Ag/Silicone ink	200 μm (diameter)	X	RT	~ 0.00001	(*5*)
	Ag ink	2 μm (diameter)	X	> 150 °C (for annealing)	1.9	(*1*)
Electro-hydrodynamic inkjet	Ag, Cu, Co inks	~ 0.7 μm (diameter)	X	150 °C (for annealing)	3.3	(*3*)
Electro-deposition	Cu, Pt	~ 0.7 μm (diameter)	X	RT	~ 32.8	(*2*)
Selective Laser Sintering	Stainless Steel	~ 100 μm (pattern width)	X	> 500 °C	N/A	(*19*)
Thermal/Piezo inkjet	Au inks	~ 30 μm (diameter)	X	~ 150 °C	~ 30	(*20*)

Table S2. Comparison with published results of liquid metal patterning in the aspect of line width, the free-standing 3D structure, reconfigurability, and the used substrate.

	Minimum line width	Free-standing 3D structure	Reconfigurability	Ref.
This work	1.9 µm	O	O	-
Direct printing	340 µm	O	X	(*24*)
	≥ 83 µm	X	X	(*30*, *36*)
Screen printing	208 µm	X	X	(*28*)
Stencil printing	≥ 10 µm	X	X	(*29*)
Microfluidic channel	20 µm	X	X	(*26*)
Transfer printing	≥ 2 µm	X	X	(*28*, *31*, *32*, *33*)
Laser patterning	100 µm	X	X	(*34*)

Movie S1. Reconfiguration of the square coil antenna. To show the relocation process in detail, the camera zooms in twice between 0:07-0:08. This video is played at 30 times faster speed.

Movie S2. Multiple reconfigurations of the EGaIn filament. Four times of the reconfiguration were done in series.

Movie S3. Reconfiguration of EGaIn that connects about a 650-μm step. The step is made by stacking two 4-inch wafers (about 525 μm thickness) and fixed with double-sided tape (100 μm thickness). To show the relocation process in detail, the camera zooms in twice between 0:07-0:08. This video is played at 30 times faster speed.

Movie S4. Formation of kink-shaped 3D structure by reconfiguration.

Movie S5. Formation of arc-shaped 3D structure by reconfiguration.

Movie S6. Breakdown procedure of EGaIn under increasing dc bias. Joule heating and the maximum temperature of EGaIn under bias are measured.

Movie S7. Breakdown procedure of EGaIn under increasing ac bias (120 Hz). Joule heating and the maximum temperature of EGaIn under bias are measured.

Movie S8. Lift-off and relocation of 3D interconnect for LED switching circuit. The step size of each LED device is 200 μm and the length of interconnect is 400 μm. This video is played at 30 times faster speed.

Movie S9. Light emission from the RGB LED array. After first switching, the emission from red LEDs is off and green LED is on. After second switching, the emission from the green LED is off and blue LED is on sequentially.

Movie S10. Light emission from selected pixels in the 4 × 4 microLED array. Each microLED pixel is interconnected by the reconfigurable 3D printing of EGaIn.